

Future Neutrino Oscillation Sensitivities for LBNE

MATTHEW BASS¹, DANIEL CHERDACK AND ROBERT J. WILSON
FOR THE LBNE COLLABORATION*Department of Physics*
Colorado State University, Fort Collins, CO, USA

The primary goal of the Long-Baseline Neutrino Experiment (LBNE) is to measure the neutrino mixing matrix parameters. The design, optimized to search for CP violation and to determine the neutrino mass hierarchy, includes a large $\mathcal{O}(10 \text{ kt})$ Liquid Argon Time Projection Chamber (LAr TPC) at 1300 km downstream of a wide-band neutrino beam. A brief introduction to the neutrino mixing parameters will be followed by a discussion of sensitivity study analysis methods and a summary of the results for LBNE. The studies include comparisons with the Tokai-to-Kamioka (T2K) and NuMI Off-axis electron-neutrino Appearance ($\text{NO}\nu\text{A}$) experiments as well as combined sensitivities. Finally, the impact of including a realistic set of systematic uncertainties will be presented.

PRESENTED AT

DPF 2013

The Meeting of the American Physical Society
Division of Particles and Fields
Santa Cruz, California, August 13–17, 2013

¹Presented by Matthew Bass at the DPF 2013 Meeting of the American Physical Society Division of Particles and Fields, Santa Cruz, California, August 13-17, 2013

1 Introduction

Neutrino flavor oscillation, or mixing, has been well established experimentally. However the parameters that describe this mixing for the three-neutrino scenario, the elements of the PMNS matrix[1][2][3], have been measured to various levels of precision. These parameters consist of three angles θ_{12} , θ_{13} , and θ_{23} , and Charge-Parity (CP) violating phase, δ_{CP} , that govern the amplitude of the mixing. The frequency of the oscillations with respect to baseline and neutrino energy is determined by the mass squared differences: Δm_{21}^2 , Δm_{31}^2 , and Δm_{32}^2 , of which two are distinct. The angles θ_{12} and θ_{23} as well as the mass squared differences have been well constrained by several neutrino experiments. The angle θ_{13} has recently been constrained by accelerator based experiments that have measured $\nu_\mu \rightarrow \nu_e$ appearance rates and reactor experiments that have measured electron-neutrino disappearance rates.

There are, however, still open questions to be answered. The value of δ_{CP} is currently not well constrained by any experiment. A non-zero value of $\sin \delta_{CP}$, signifying a CP violating process, would mean that neutrinos and anti-neutrinos mix differently. Although current experimental data is consistent with maximal mixing for θ_{23} , if more precise measurements find θ_{23} to be less than maximal then $\nu_\mu \rightarrow \nu_e$ oscillations will be sensitive to the θ_{23} octant. Finally, while the values of Δm_{21}^2 and $|\Delta m_{31}^2|$ are known[5] within 3%, the sign of $|\Delta m_{31}^2|$, or the neutrino mass hierarchy, is unknown. A positive(negative) value is denoted the normal(inverted) hierarchy.

An approximate form[4] for the probability of $\nu_\mu \rightarrow \nu_e$ in matter is

$$\begin{aligned}
P_{\nu_\mu \rightarrow \nu_e} \approx & \sin^2 2\theta_{13} \sin^2 \theta_{23} \frac{\sin^2((1-x)\Delta)}{(1-x)^2} \\
& - \alpha \sin 2\theta_{13} \sin \delta \sin 2\theta_{12} \sin 2\theta_{23} \sin \Delta \frac{\sin(x\Delta)}{x} \frac{\sin((1-x)\Delta)}{(1-x)} \\
& + \alpha \sin 2\theta_{13} \cos \delta \sin 2\theta_{12} \sin 2\theta_{23} \cos \Delta \frac{\sin(x\Delta)}{x} \frac{\sin((1-x)\Delta)}{(1-x)} \\
& + \alpha^2 \cos^2 \theta_{23} \sin^2 2\theta_{12} \frac{\sin^2(x\Delta)}{x^2},
\end{aligned} \tag{1}$$

where $x = \frac{2\sqrt{2}G_F N_e E}{\Delta m_{31}^2}$, $\Delta = \frac{\Delta m_{31}^2 L}{4E}$, and $\alpha = \frac{\Delta m_{21}^2}{\Delta m_{31}^2} \approx 0.03$. All six of the parameters governing neutrino oscillations appear in this equation. The current constraints on the oscillation parameters still allow for functionally degenerate solutions to Eq. 1. Figure 1 shows schematically how these degeneracies arise at a baseline (L) of 1300 km by plotting the probabilities for ν_e appearance as a function of neutrino energy. For example, a variation of δ_{CP} from 0 to $-\pi/2$ resembles a variation of $\sin^2 \theta_{23}$ from 0.5 to 0.6. So there is a functional degeneracy between the two parameters. An experiment with sufficient energy resolution, statistics, and understanding of systematic

uncertainties will be required to disentangle their effects.

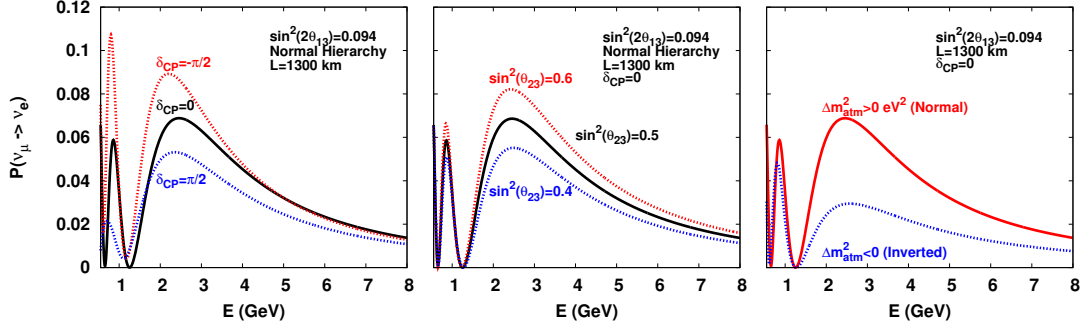


Figure 1: Probabilities for $\nu_\mu \rightarrow \nu_e$ as a function of neutrino energy for variations in δ_{CP} (left), $\sin^2 \theta_{23}$ (middle), and mass hierarchy (right) at 1300 km.

2 LBNE

The LBNE[6] is currently designed with a 700 kW wide-band muon-neutrino beam from the Fermi National Accelerator Laboratory (FNAL) to the Sanford Underground Research Facility (SURF). At a baseline of 1300 km from the beam source, a massive liquid argon TPC will be built underground. Also planned is a near detector, at FNAL, capable of reducing systematics to levels comparable with the assumptions used in these studies.

LBNE is planning for a staged construction. In one scenario, LBNE10 will have a 10 kt fiducial mass LAr TPC with a 700 kW, 120 GeV beam. The proposed LBNE has a 34 kt fiducial mass LAr TPC, underground with a 700-2300 kW beam (see Project X[7]) in addition to a near neutrino detector at FNAL.

With its optimized 1300 km baseline, LBNE will further constrain θ_{23} , determine the θ_{23} octant (for $\theta_{23} \neq 45^\circ$), determine the mass hierarchy, and detect CP violation for previously unreachable regions of the neutrino oscillation parameter phase space. This work focuses on the physics goals obtainable through ν_e appearance and ν_μ disappearance analyses. There are many other physics goals for LBNE which are outlined in [6].

3 Method for Estimating Sensitivity

Sensitivities are computed using the GLoBES[8][9] library. Event spectra for LBNE and LBNE10 are simulated using parameterizations[6] of the flux, cross sections, energy resolutions, and analysis sample selection efficiencies. Event spectra for ν

and $\bar{\nu}$ modes in both ν_e appearance and ν_μ disappearance are considered. A $\Delta\chi^2$ is computed comparing a true event spectrum with test hypothesis spectra. The $\Delta\chi^2$ is minimized with respect to oscillation parameter uncertainties, adapted from the Fogli et al. 2012 global fit[5], and normalization uncertainties of 1% on signal and 5% on background events. For these studies, LBNE and LBNE10 are assumed to run with equal periods of ν and $\bar{\nu}$ running.

4 LBNE Sensitivity

Figure 2 gives the expected resolution on δ_{CP} , in degrees, as a function of the true value of δ_{CP} where the mass hierarchy is assumed to be known to be the normal hierarchy. LBNE10 will measure δ_{CP} to $\sim 17^\circ$ in the best case and $\sim 31^\circ$ in the worst case. The full LBNE, at 34 kt, will be able to measure the δ_{CP} resolution to between 10° and 17° . The right panel of Fig. 2 shows how these resolutions improve for two values of δ_{CP}^{true} as a function of exposure in kt·MW·years and for various uncertainties on signal and background normalizations. Uncertainties in the shape of the reconstructed energy spectra are not considered for these studies. These results depend upon the assumptions made concerning the systematic uncertainties on signal and background. The effect of varying these uncertainties can be seen in Fig. 2. More detailed treatments of systematic uncertainties are being considered within the context of the LBNE Fast Monte Carlo simulation[6].

Figure 3 illustrates the sensitivity of LBNE10 and LBNE to CP violation. The left panel shows the values of $\sin^2 \theta_{23}$ and δ_{CP} for which CP violation can be observed at the 3σ level. LBNE10 will have 3σ sensitivity for a significant fraction of δ_{CP} values if $\sin^2 \theta_{23}$ is in the lower octant. LBNE will have significant sensitivity for all $\sin^2 \theta_{23}$ values. The right panel of Fig. 3 shows the sensitivity, in σ , to which LBNE10 and LBNE can detect CP violation as function of the true value of δ_{CP} , for the case in which $\sin^2 \theta_{23}$ is equal to the global best-fit value[5]. CP violation can be detected at the 3σ level for 40% of δ_{CP} values with LBNE10 and 67% of δ_{CP} values with LBNE.

Figure 4 shows the performance, in terms of $\Delta\chi^{2*}$, for LBNE10 and LBNE in determining the neutrino mass hierarchy. The $\Delta\chi^2 \geq 9$ regions where the mass hierarchy can be determined show nearly complete coverage for LBNE10 and complete coverage for LBNE. The sensitivity as a function of δ_{CP} shows that LBNE10 can determine the mass hierarchy at $\Delta\chi^2 \geq 9$ for most δ_{CP} values while LBNE has nearly complete δ_{CP} coverage for mass hierarchy determination with $\Delta\chi^2 \geq 25$.

Studies, not shown here, were also done to assess the sensitivity added by including information from T2K and NO ν A. In LBNE10, a combined fit to LBNE10, T2K, and

*Qian et al. [12] have shown that the probability of correct mass hierarchy determination is not correctly described by frequentist statistical methods, and provide a method for properly calculating them based on these results.

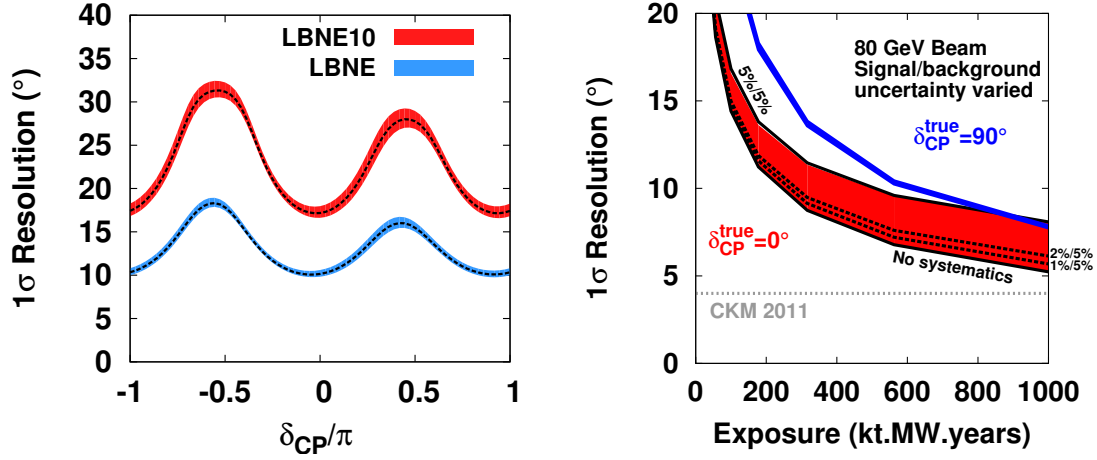


Figure 2: (left) Expected 1σ resolution on δ_{CP} for LBNE10 and LBNE. The bands represent current uncertainties on θ_{23} and Δm_{31}^2 and projected uncertainties on θ_{13} from the Daya Bay experiment. The mass hierarchy is assumed to be known and normal. (right) Expected 1σ resolution on δ_{CP} as a function of exposure for $\delta_{CP} = 0^\circ$ (red) and $\delta_{CP} = 90^\circ$ (blue) for multiple assumptions on signal and background normalization uncertainties. The level of precision of measurements for the CKM matrix describing quark mixing is given for comparison.

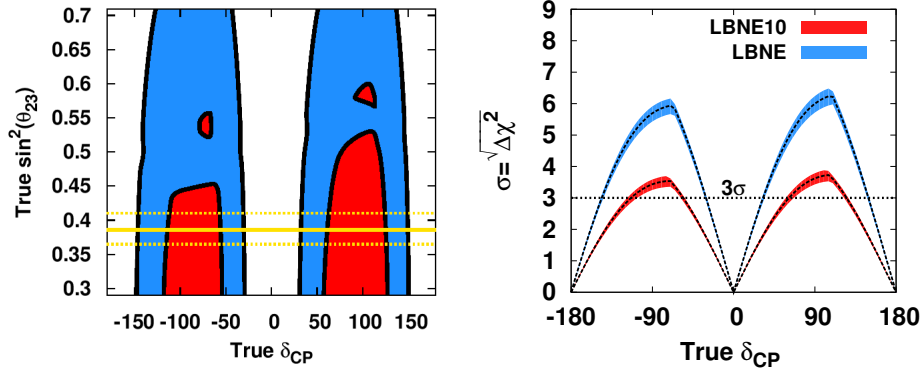


Figure 3: CP violation sensitivity assuming true normal hierarchy. (left) Regions in $\sin^2 \theta_{23}$ vs. δ_{CP} where LBNE (cyan) and LBNE10 (red) have 3σ sensitivity to CP violation. The central value(1σ range) on $\sin^2 \theta_{23}$ from the Fogli et al. 2012 global fit are indicated with the solid(dashed) yellow lines. (right) Expected sensitivity, in σ , with which LBNE and LBNE10 will be able to determine CP violation at $\sin^2 \theta_{23} = 0.39$. The bands represent current uncertainties on θ_{23} and Δm_{31}^2 and projected uncertainties on θ_{13} .

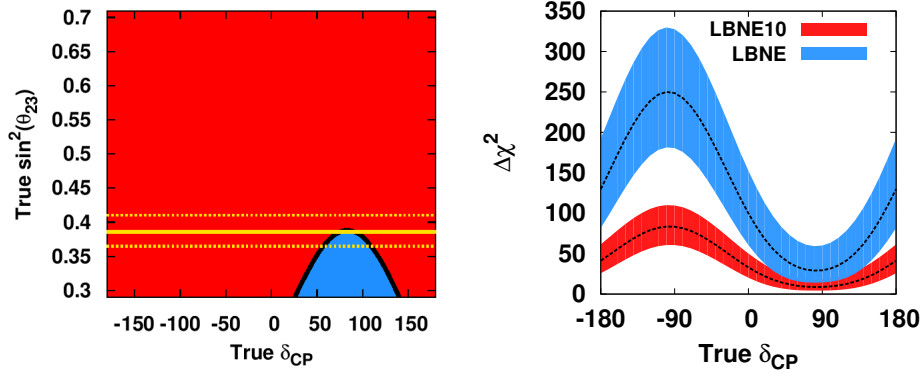


Figure 4: Mass hierarchy sensitivity assuming true normal hierarchy. (left) Regions in $\sin^2 \theta_{23}$ vs. δ_{CP} where LBNE (red and cyan) and LBNE10 (red) have $\Delta\chi^2 \geq 9$ for the normal mass hierarchy. The central value(1σ range) on $\sin^2 \theta_{23}$ from the Fogli et al. 2012 global fit are indicated with the solid(dashed) yellow lines. (right) Expected sensitivity, in $\Delta\chi^2$, with which LBNE and LBNE10 will be able to determine the mass hierarchy at $\sin^2 \theta_{23} = 0.39$. The bands represent current uncertainties on θ_{23} and Δm_{31}^2 and projected uncertainties on θ_{13} .

NO ν A provides a significant boost to the sensitivity. For example, for the worst case mass hierarchy sensitivity (around $\delta_{CP} = 90^\circ$ in the normal hierarchy) the $\Delta\chi^2$ improves from ~ 9 to ~ 16 . However, for high exposures in LBNE, the combined, T2K+NO ν A+LBNE fit contributes little over LBNE alone to the sensitivity.

5 Conclusion

LBNE will be a major step forward in ability to constrain the neutrino oscillation parameters of the PMNS matrix. Even early stages of the experiment, characterized here by LBNE10, represent a large improvement on current and near-future neutrino oscillation measurements. With the assumptions outlined here, LBNE will be able to measure δ_{CP} to between 10° and 20° , detect CP violation at 3σ for 67% of δ_{CP} values, and resolve the neutrino mass hierarchy with $\Delta\chi^2 \geq 25$.

References

- [1] B. Pontecorvo, Sov. Phys. JETP **6**, 429 (1957) [Zh. Eksp. Teor. Fiz. **33**, 549 (1957)].

- [2] B. Pontecorvo, Sov. Phys. JETP **26**, 984 (1968) [Zh. Eksp. Teor. Fiz. **53**, 1717 (1967)].
- [3] Z. Maki, M. Nakagawa and S. Sakata, Prog. Theor. Phys. **28**, 870 (1962).
- [4] M. Freund, M. Lindner, S. T. Petcov and A. Romanino, Nucl. Phys. B **578**, 27 (2000) [hep-ph/9912457].
- [5] G. L. Fogli, E. Lisi, A. Marrone, D. Montanino, A. Palazzo and A. M. Rotunno, Phys. Rev. D **86**, 013012 (2012) [arXiv:1205.5254 [hep-ph]].
- [6] C. Adams *et al.* [LBNE Collaboration], arXiv:1307.7335 [hep-ex].
- [7] A. S. Kronfeld, R. S. Tschirhart, U. Al-Binni, W. Altmannshofer, C. Ankenbrandt, K. Babu, S. Banerjee and M. Bass *et al.*, arXiv:1306.5009 [hep-ex].
- [8] P. Huber, M. Lindner and W. Winter, Comput. Phys. Commun. **167**, 195 (2005) [hep-ph/0407333].
- [9] P. Huber, J. Kopp, M. Lindner, M. Rolinec and W. Winter, Comput. Phys. Commun. **177**, 432 (2007) [hep-ph/0701187].
- [10] M. D. Messier (1999), Ph.D. Thesis (Advisor: James L. Stone).
- [11] [35] E. Paschos and J. Yu, Phys.Rev. D65, 033002 (2002), hep-ph/0107261.
- [12] X. Qian, A. Tan, W. Wang, J. J. Ling, R. D. McKeown and C. Zhang, Phys. Rev. D **86**, 113011 (2012) [arXiv:1210.3651 [hep-ph]].